Gold Nanostructures by Directional Solid-state Decomposition

Srdjan Milenkovic, André Schneider, Achim Walter Hassel
Max-Planck-Institut für Eisenforschung GmbH, Max-Planck-Strasse 1, 40237 Düsseldorf, Germany

Abstract

This study addresses a novel approach of obtaining gold nanostructures, via directional eutectoid decomposition and selective etching of Fe-Au alloys. The eutectoid transformation occurs at 2.3%Au, which agrees perfectly with existing DTA and calculated data. The results are thus experimentally supporting the calculated part of the binary Fe-Au phase diagram. Gold nanofibres were rectangular in shape, constrained with two perpendicular crystallographic directions, showing the faceted nature of the Au phase. In addition, it was shown that a range of gold nanostructures, including gold nanoparticles, short nanorods, and nanofibres might be achieved depending on the processing route. The uniformity and regularity of the obtained nanostructures are limited, due to a non-cooperative mechanism of the eutectoid transformation. These homomorph gold nanostructures have the same high potential as other gold nanostructures but also the advantage of being inherently organized in a single crystalline matrix.

Keywords

Gold nanostructures, directional solidification, phase transformation, nanotechnology.

Introduction

The trend in electronics industry towards miniaturisation is leading to increasing research focus on nano-electronic devices. For example, metal nanowires show potential for future application as connector lines in such devices. The controlled fabrication of these structures at scales beyond the current limits of lithographic techniques is of great interest. Self–assembly processes using gold nanoparticles are being extensively studied as one possible long-term solution. This study addresses a novel approach of obtaining gold nanostructures. It consists of applying directional solidification processing to eutectoid alloys in order to produce ordered structures, followed by phase separation by selective etching.

The directional transformation of eutectoid alloys is a close derivation of the directional solidification of eutectics. In this case, two phases precipitate simultaneously from a high-temperature solid phase (Figure 1). When the growth properties of the two phases are sufficiently compatible, unidirectional decomposition can also produce aligned composite materials [1, 2]. One of the most prominent examples of eutectoid reaction is the formation of pearlite by undercooling a Fe-C alloy in the γ-state. Microstructures are best when the high-temperature phase is nearly single-crystalline. Therefore, aligned eutectoids are often produced by accomplishing unidirectional solidification and unidirectional decomposition sequentially. Eutectic solidification and eutectoid decomposition, as examples of duplex crystal growth, are inherently more complex than single-phase crystal growth. The technique used in both cases is quite similar: a specimen is unidirectionally translated through a steep temperature gradient and traversed by a macroscopically planar transformation front. If adequate experimental conditions are arranged, the eutectoid reaction product is an aligned microstructure. The conditions to be met are: i) sufficiently steep gradient to avoid both nucleation before the actual position of the transformation front and coalescence afterwards, ii) a translation rate which permits the attainment of a transformation front with stationary moving conditions, i.e., as a first approximation, a lower translation rate than the maximum eutectoid growth rate.

Although eutectic and eutectoid reactions are essentially the same in nature, there are some differences that must be pointed out. Firstly, eutectoid spacings are much finer than the eutectic spacings for the same growth rate, due to the lower values of diffusion coefficients in the solid state as compared to the liquid. Also, a decrease in eutectoid spacing, λ, with increasing growth rate, V, is generally slower for eutectoids than for eutectics. Data can again be fitted to a formula $\lambda^n V = \text{const}$. However, whereas $n = 2$ fits to almost all data for eutectics, values of n ranging from 2 to 4 have been reported for eutectoids. The value $n = 2$ is consistent with volume-diffusion control, and $n = 3$ is predicted for grain-boundary-diffusion control. Carpay and Van Den

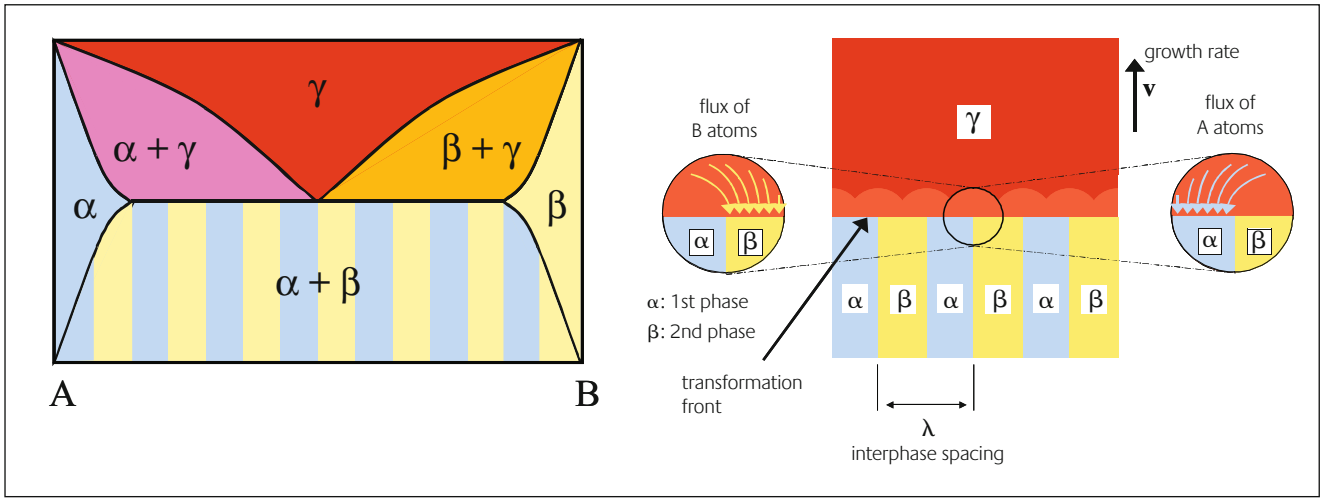

Figure 1
Schematic of directional eutectoid decomposition

Boomgaard [3, 4] have developed a boundary-diffusion model in which growth rate is limited by atom attachment kinetics, an effect ignored in other models. Their model gives $n = 4$, in agreement with their experimental results on several alloys. Chadwick [5] has also shown that kinetic contributions to undercooling can yield n values greater than 3.

Moreover, directional decomposition at off-eutectoid compositions can lead to the formation of coarse pro-eutectoid particles, the equivalent of dendrites in off-eutectic solidification. However, Chadwick and Edmonds [6] have shown that the composition range for composite growth increases with increasing growth rate, in agreement with coupled growth theories. Despite considerable information has been gathered up to date, it should be mentioned that aligned eutectoids are in a much earlier stage of study than aligned eutectics, and that their properties and potential applications have been evaluated to a much lesser extent.

Fe-Au phase diagram

In order to obtain gold nanofibres, we pursued a binary system, which exhibits a eutectic-like reaction with Au as a minor phase (< 10%), leading to a fibrous morphology of gold. Interestingly, among a large number of existing binary Au diagrams only the Fe-Au diagram met the requirement.

Figure 2 represents the phase relationships in the system Fe-Au, constructed from data reported in the literature [7-13]. The diagram is based mainly on experimental results obtained by Raub and Walter [9] and Buckley and Hume-Rothery [12]. More recently, Okamoto et al. assessed the phase diagram [14]. The equilibrium phases are: liquid, fcc terminal solid solutions of Au and γ-Fe, and bcc terminal solid solutions of δ-Fe and α-Fe. There are no intermetallic compounds in this system. The intermediary phase Fe_3Au reported in earlier investigations has not been confirmed [10-13]. The Au-rich part of the phase diagram has interested a number of investigators due to magnetic properties of Au-rich Fe-Au alloys. The influence of ordering, spin orientation, impurities etc. have been studied by Wenger and Keesom [15], Dawes and Voles [16], Murani [17], Smith and Liu [18], and de Mayo [19]. Resistivity measurements and electron microscopy [20] and metallographic analysis [21] have achieved a lot to clarify the morphology and kinetics of precipitation in Fe-Au alloys.

In the Fe-rich region, addition of Au increases the α/δ-Fe transformation temperature [12], but decreases that of the α/γ-Fe transformation. The maximum solid solubility of Au in δ-Fe was found to be 2.3 at% at 1431 °C and in γ-Fe 4.1 at% at 1171 °C. The solid solubility data of Au in α-Fe for the temperature range 500–903 °C are taken from X-ray measurements of [9] and are in a good agreement with values reported by [13]. The reported solid solubilities of Au at 500 °C were 0.14 at% [9] and 0.1 at% [13], respectively. The maximum solubility of Au in α-Fe is placed at 2.2 at% Au

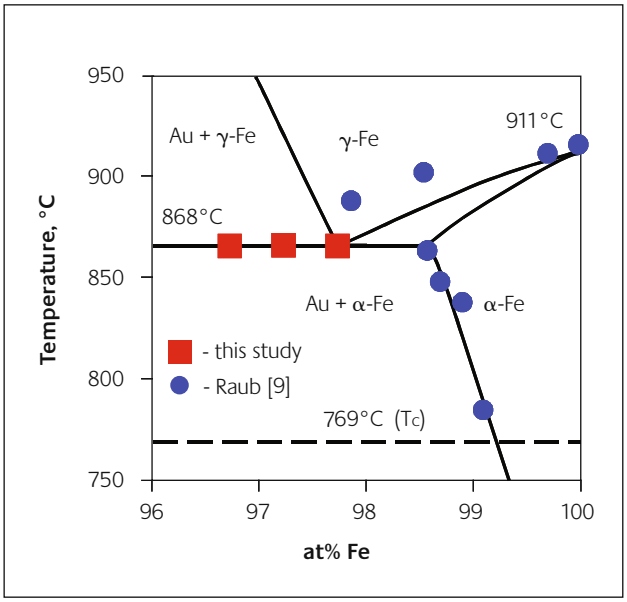

Figure 2
Fe-rich part of the Fe-Au binary phase diagram

at 903°C [9]. Considering the γ-Fe → α-Fe + Au eutectoid reaction, the data are rather scarce. Seigle [11] placed the transformation temperature at 860 ± 5°C. Jette et al. [10] found that alloys quenched from 894°C showed the γ-Fe diffraction lines, and concluded that the transformation temperature must be below 894°C. An estimate of this temperature, according to the thermodynamic model of Okamoto et al. [14], showed a value of 868°C, which is close to that of Seigle [11] and consistent with that of Jette [10]. The low eutectoid temperature of about 830°C observed by Isaac [7] is likely to be caused by supercooling. The composition of the eutectoid reaction reported by Raub [9] was 2.3 at% Au and that calculated by Okamoto 2.2 at% Au, exhibiting good agreement.

The present study addresses preparation of gold nanostructures via directional solid-state decomposition. The main objectives are to evaluate the suitability of a eutectoid transformation in the Fe-Au system for obtaining gold nanofibres and nanofibre arrays and to study the effect of composition and processing conditions on the microstructure and morphology.

Experiments

Pre-alloys were prepared using 99.999%Au and Fe, which was 5 times zone refined in house, by induction melting under inert atmosphere and drop casting into a cylindrical copper mould. Subsequently, the as-cast ingots were inserted into alumina crucibles and processed in a Bridgman type crystal growing facility. It consists of the crucible support, cooling ring and heating element (Tungsten net). The alumina crucible with the as-cast ingot was positioned in the furnace and heated up to ~1600°C. After the material in the crucible was completely melted, the upper part with the heating element is slowly and uniformly shifted upwards, providing thus unidirectional heat extraction. This operation is controlled by a servomotor that enables a speed range from 1 to 200 mm/h. The experiments were conducted at a temperature of 1600 ± 10°C, a thermal gradient of approximately 40 K cm^{-1} and a growth rate of 30 mm h^{-1}.

The selective etching of the α-Fe phase in the alloy was achieved after digestion of the sample into a solution containing 3.2% HCl in distilled water. The eutectoid alloy was cut in 1x1x0.1 cm pieces, which were then immersed into the solution and left stirring overnight. The reddish solution obtained with this treatment was analysed by ICP-OES (inductively coupled plasma optical emission spectroscopy) in order to calculate the total content of the Fe and Au. All solutions were prepared from p.a. grade chemicals and high purity water (Millipore filter system). All materials used were of analytical grade and purchased by Merck (Darmstadt, Germany).

Scanning electron microscopy pictures were obtained using a high resolution scanning electron microscope with a field emission gun (Leo 1550 VP apparatus, Leo Elektronenmikroskopie GmbH, Oberkochem, Germany) fitted with an INCA Energy Dispersive System (EDS) (Oxford Instruments, Oxford, UK).

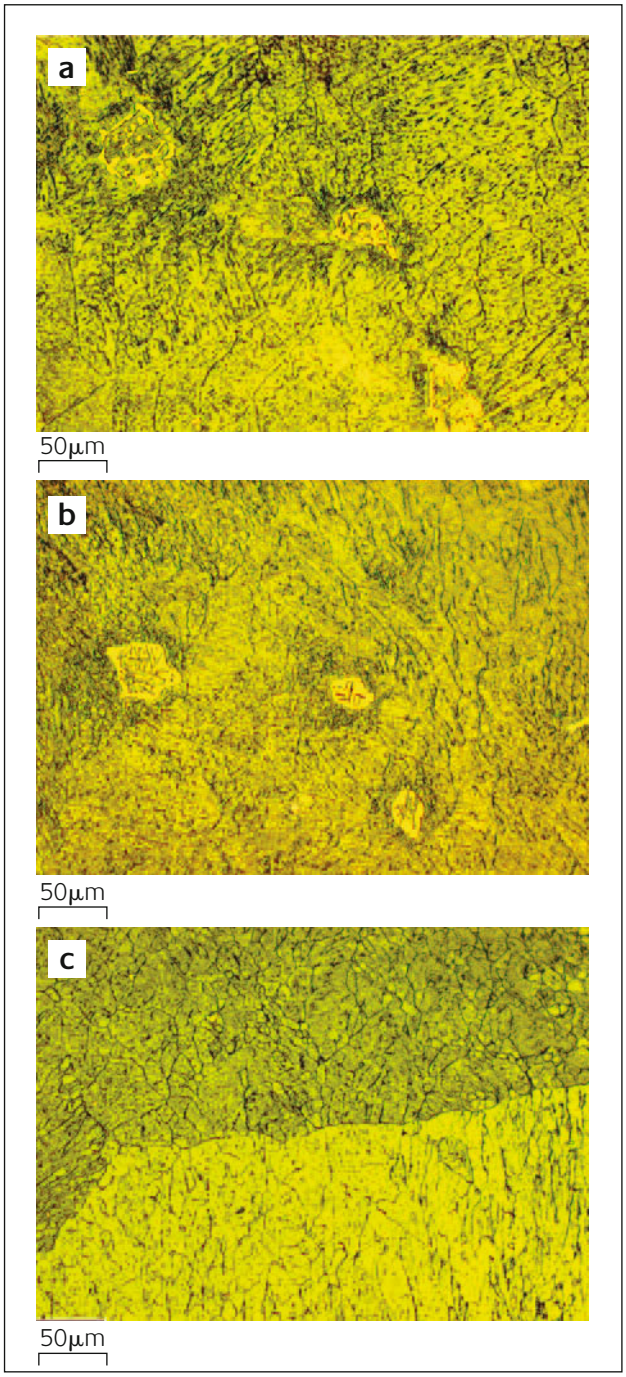

Figure 3
Microstructure of the: a) Fe-2.7 %Au; b) Fe-3.2 %Au; and c) 2.3 %Au alloys (light optical microscopy)

Results and Discussion

Effect of the composition

Since the literature data on the eutectoid composition in the Fe-Au system are based on DTA measurements and thermodynamic optimisation, we selected three alloy compositions with the aim to confirm the exact composition.

Table 1

Nominal and measured compositions of the investigated alloys

	Nominal				ICP-OES			
Alloy	**At%**		**Wt%**		**At%**		**Wt%**	
	Fe	Au	Fe	Au	Fe	Au	Fe	Au
1	97.7	2.30	92.35	7.65	97.78	2.28	92.60	7.40
2	97.3	2.70	91.10	8.90	97.27	2.73	91.00	9.00
3	96.8	3.20	89.56	10.44	96.78	3.22	89.50	10.50

Table 1 shows nominal compositions of the alloys and measured ones by ICP-OES. They show good agreement, indicating that homogeneous alloys with precise chemical compositions were obtained. Typical microstructures after directional solidification were coarse grained with a grain size ~1.5 ± 0.5mm. The microstructure of alloys with 2.7 and 3.2 %Au (percents throughout the paper are atomic) was very fine and generally consisted of proeutectoid phase embedded in a eutectoid microstructure. The proeutectoid grains could be recognized as bright regions roundly shaped in the interior of the old grains (Figure 3a-b). At higher magnifications, it turned out that the bright regions are nearly free of sub-boundaries. In the interior of the grains, the presence of small plate-like precipitates (about 5 nm thick, 50 nm long) has been observed by SEM. From EDS, they have been identified as Fe-rich bcc precipitates embedded in a Au fcc matrix.

On the other hand, the alloy with 2.3%Au (Figure 3c) exhibited an entirely eutectoid structure without any traces of proeutectoid phase, indicating that this is the exact eutectoid composition for the applied growth conditions. The microstructure consisted of sub-boundaries and dislocation networks, most of which were introduced by the $\gamma \rightarrow \alpha$ transformation during the thermal history of the alloy. Also, the light optical micrographs indicated that the sub-boundaries play an important role in precipitate nucleation, but the details of the process could be better followed by SEM and are described in the next section.

Effect of the processing conditions

In order to investigate the influence of the processing conditions on the microstructure and morphology, the alloy with 2.3% was submitted to three different processing routes as described in the experimental part. In all cases the microstructure consisted of grains with networks of sub-boundaries. However, in the interior the morphology comprised iron matrix with gold precipitate, which showed to be prone to previous thermal history, i.e., the processing route of the alloy.

Directionally solidified samples exhibited very fine Au precipitates in the α-Fe matrix, which is typical for the continuous precipitation from the saturated solid solution upon cooling. This suggests that the eutectoid reaction was suppressed. One of the possible explanations is that the growth rate employed was larger than the critical one. Successful directional eutectoid decomposition not only requires large grain size and high temperature gradient, but is also limited by the existence of a maximum rate of coupled growth in each system. Samples grown faster than this limiting rate yield unaligned structures or may even result in other transformation modes, which presumably occurred in this case. Further, a closer insight into the particle distribution and morphology after selective etching of the matrix (Figure 4), permitted an analysis of the nucleation mechanism of the particles. The mechanism of nucleation depends on the strain energy needed for the formation of the new phase. When the atomic volume of matrix and precipitate atoms are approximate, the nucleation of particles requires little strain energy and therefore, the nucleation barrier is determined only by the surface energy between the particle and the

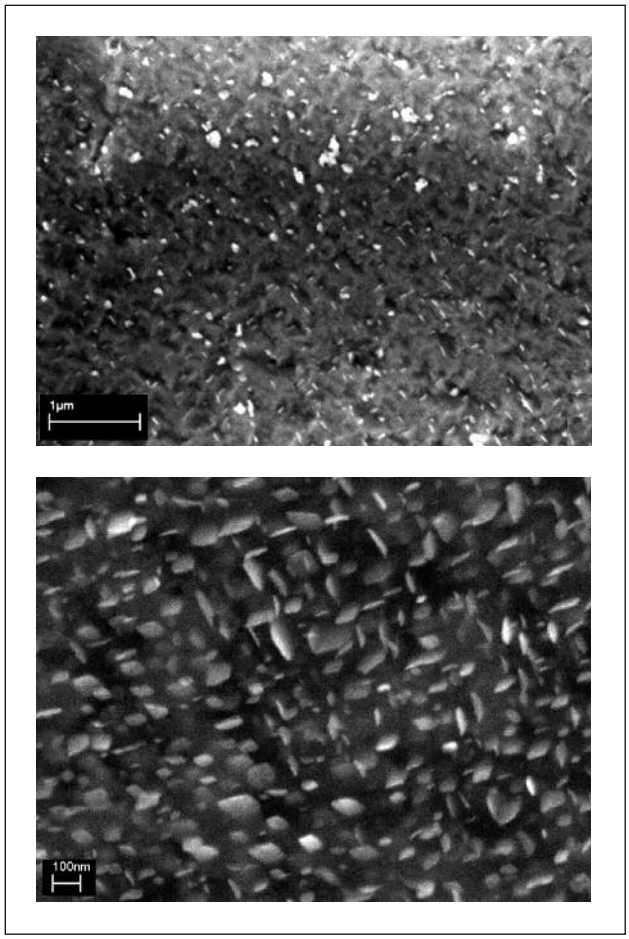

Figure 4

Microstructure of the directionally solidified Fe-2.3 %Au alloy (SEM micrograph in the BSE mode)

matrix. In this case there is no tendency towards preferred nucleation on lattice imperfections. On the other hand, if solute atoms and the precipitate phase differ significantly in volume from solvent atoms and the matrix, there is a tendency for the solute atom to segregate to a dislocation, but this requires an additional strain energy to form a nucleus of critical size. Hence, small clusters of atoms may grow, but they are not able to exceed the critical nucleus size. Therefore, dislocations must be present to achieve nucleation. In this case, the precipitates are plate-shaped and lie on definite habit planes. Such a morphology was observed in the directionally solidified sample as depicted in Figure 4, indicating that the precipitation of the Au particles occurs on the dislocations, due to a large strain energy caused by the enormous difference between the atomic volumes of the α-Fe and the Au atoms. Hence, this processing route could be used for production of gold nanoparticles, which could easily be extracted from the matrix.

The sample that was cooled down from the liquid just below the solidus line and kept for four hours at 1330°C and then moved down along a temperature gradient consisted of gold fibres partially aligned along the several crystallographic directions, as depicted in Figure 5. The morphology of the fibres was rectangular rather than circular. In an early work on single-phase materials, Jackson [22] distinguished between 'non-faceted' phases that solidify with complete crystallographic isotropy via an atomically rough solid/liquid interface, and 'faceted' phases that have preferred crystallographic growth directions associated with atomically smooth solid/liquid surface facets. The presence of fibres with rectangular shape, which are constrained with two perpendicular crystallographic directions (Figure 5) clearly indicate the faceted nature of the Au phase. The faceted morphology of the fibres can be explained from an energetic point of view. The energy of an individual precipitate particle is a sum of the elastic strain energy due to the lattice mismatch between precipitate and the matrix phase, E_{str}, surface energy of precipitate E_{surf} and elastic interaction energy between precipitates, E_{int}. In the case of eutectic and eutectoid precipitation, the particles are far away from each other, so the E_{int} can be regarded as zero. Hence, the shape of the precipitate is determined by minimizing the sum of E_{str} and E_{surf}. In order to minimize the interface energy eutectic phases develop a preferred crystallographic orientation relationship between each other. Since for some crystallographic orientations the surface energy is isotropic and anisotropic for others, the shape of the particles depends on the surface energy for the given crystallographic orientation relationship. Hence, it is clear that for the existing crystallographic orientation relationship between α-Fe and Au, the surface energy of the Au fibres is anisotropic.

As it may be seen on Figure 5, the fibres are not regularly distributed and are only partially aligned. This indicates that the conditions for the steady state growth were not reached. The reason for that might be the initial microstructure. The microstructure of the resulting eutectoid phases is sensitive to

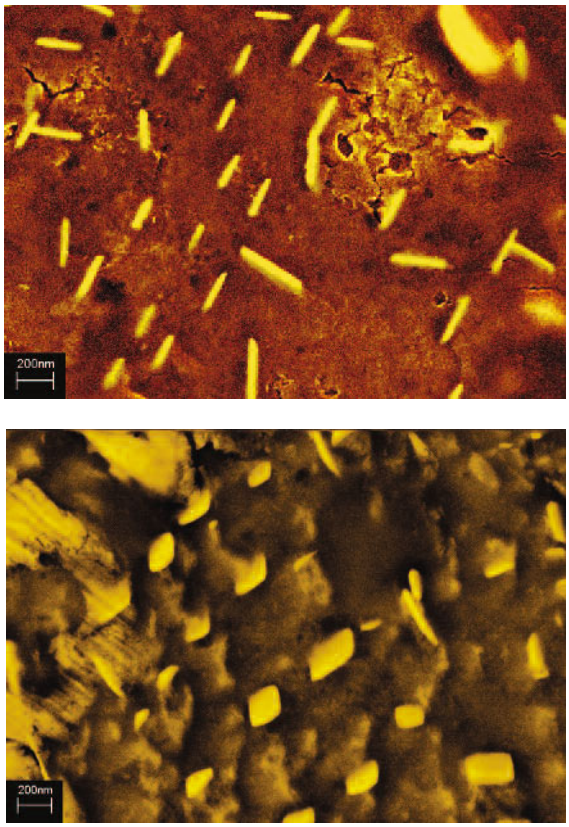

Figure 5
Microstructure of the solidified and heat treated Fe-2.3 %Au alloy (SEM micrograph in the BSE mode)

the initial structure and homogeneity of the high-temperature phase, and therefore to the solidification conditions of that phase. If the high-temperature phase is fine-grained, this usually limits the ultimate size of the eutectoid phase [6, 23] and the degree of phase alignment [1]. This is presumably because the grain boundaries ahead of the advancing transformation front serve as nuclei for new, generally unaligned, eutectoid grains. Carpay [1] suggested the finer the grain size of the high-temperature phase, the higher is the temperature gradient necessary to suppress unwanted nucleation and maintain an aligned eutectoid structure. Considering that the sample after solidification was annealed for 4 hours at 1330°C, it is likely that the grain size was not large enough to enable the formation of well-aligned fibres. Another possibility is that the temperature gradient was not steep enough. It is well known that one of the differences between eutectics and eutectoids is that eutectoids require much higher undercooling, and consequently higher temperature gradients. The temperature gradient not only influences nucleation ahead of the interface, but also, as in the eutectic, influences the stability of a planar interface. Since the variation of velocity with temperature is much slower than for the eutectics, it is more difficult to maintain a planar eutectoid interface. Compositional or structural inhomogeneities in the high temperature phase, or stresses induced by the transformation, could also contribute to a nonplanar interface.

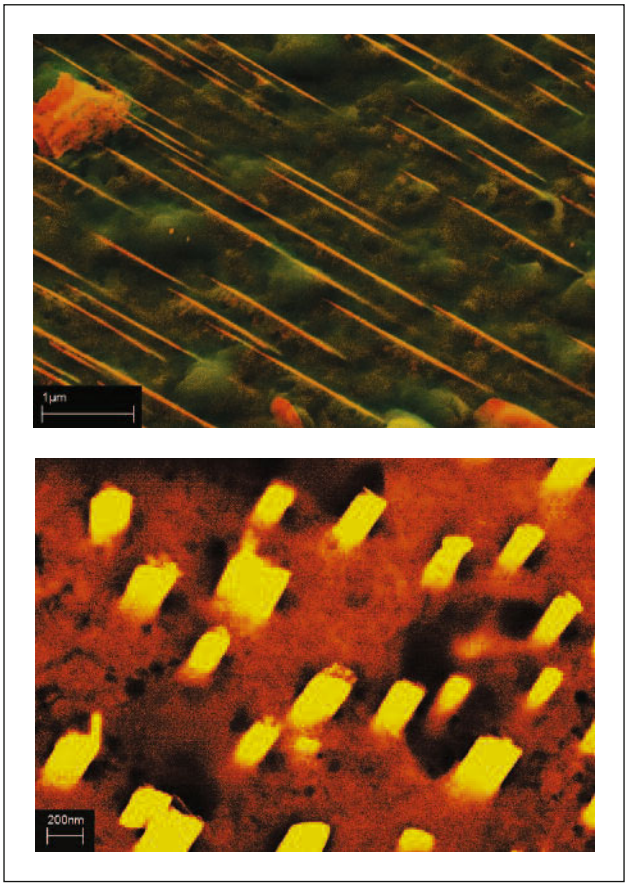

Figure 6
Microstructure of the directionally solidified and heat treated Fe-2.3 %Au alloy (SEM micrograph in the BSE mode)

Heat treatment after the directional solidification led to a cell microstructure with aligned fibres within the cells (Figure 6). This means that only this processing route ensured all the necessary conditions for aligned eutectoid decomposition. Although fibres show only one variant of the orientation relation, they are not of uniform length. This means that not all the fibres are in direct contact with austenite during the growth process, suggesting that the growth mechanism is not cooperative and occurs by repeated re-nucleation of the gold fibres. This mechanism is characteristic for the eutectoid decomposition in which the growth rate of the major constituent phase is larger than that of the minor phase. Under this condition, the minor phase is able to grow alongside the major phase only for some limited distance until it is finally overwhelmed by the neighbouring major phase and denied further access to the austenite. In that case, distance and alignment of fibres are governed by the rate of re-nucleation of the minor phase. As the re-nucleation rate decreases, the distance becomes larger and the degree of the alignment of the successively formed fibres diminishes. Microstructures of this type have already been observed in steel by Hillert [24], who termed them as the product of "a low degree of cooperation". They are also observed in hypoeutectoid [25], eutectoid [26] and hypereutectoid Ti-X alloys [27], as well as in eutectoid βCu-Al and βCu-In alloys [28].

The etching of the ds-Fe-Au alloys demonstrated that a preferential dissolution of the iron matrix is possible. For larger structures such as nanowires of Re or W formed from directional solidification of a eutectic alloy it was possible to isolate single wires with diameters of down to 100 nm [29-31]. For preparing isolated Au nanostructures from the processed material a selective dissolution process must be employed that allows a simultaneous stabilisation of the Au nanoparticles and to prevent irreversible coagulation of these particles. This is the subject of an ongoing project.

Summary

Directional solid-state decomposition in the Fe-Au system has been investigated as a new route of preparing gold nanostructures. Experimental observations of the microstructure showed that the eutectoid composition is 2.3 %Au, which agrees perfectly with DTA and calculated data from the literature [14]. In addition, the influence of several processing routes on the final microstructure was studied. It was shown that a range of gold nanostructures, including gold nanoparticles, short nanorods, and nanofibres might be achieved by this method. Finally, the observed results suggest that the mechanism of the eutectoid transformation is non-cooperative, which is responsible for the limited uniformity and regularity of the obtained nanostructures.

Acknowledgements

The financial support of the Deutsche-Forschungs-Gemeinschaft through the project *Production of Nanowire Arrays through Directional Solidification and their Application* within the DFG Priority Programme 1165 *Nanowires and Nanotubes – From Controlled Synthesis to Function* is gratefully acknowledged.

References

1 F.M.A. Carpay, *J. Cryst. Growth*, 1971, **18**, 124
2 J.D. Livingstone, in: R.W. Kraft (Ed.), Conference on In Situ Composites, National Academy of Sciences, Washington D.C., 1973, 87
3 F.M.A. Carpay, *Acta Metallurgica*, 1972, **20**, 929
4 F.M.A. Carpay, J. Van Den Boomgaard, *Acta Metallurgica*, 1971, **19**, 1279
5 G.A. Chadwick, in: R.W. Kraft (Ed.), Conference on In Situ Composites, National Academy of Sciences, Washington D.C., 1973, 25
6 G.A. Chadwick, D.V. Edmonds "Chemical Metallurgy of Iron and Steel" Iron and Steel Institute, London, 1973, 264
7 E. Isaac, W. Tammann, *Z. Anorg. Chem*., 1907, **53**, 291
8 M. Fallot, *Ann. Phys*., 1936, **6**, 376
9 E. Raub, P. Walter, *Z. Metallkd*., 1950, **41**, 234
10 E.R. Jette, W.L. Brunner, F. Foote, *Trans. AIME*, 1934, **111**, 354
11 L.L. Seigle, *Trans. AIME*, 1956, **206**, 91
12 R.A. Buckley, W. Hume-Rothery, *J. Iron Steel Inst*, 1963, **201**, 121

13 P. Royen, H. Reinhardt, *Z. Anorg. Allg. Chem*., 1955, **281**, 18
14 H. Okamoto, T.B. Massalski, L.J. Swartzendruber, P.A. Beck, *Bull. Alloy Phase Diagrams*, 1984, **5**, 592
15 L.E. Wenger, P.H. Keesom, *Phys. Rev*., 1975, **B11**, 3497
16 D.G. Dawes, B.R. Coles, *J. Phys. F: Met. Phys*., 1979, **9**, L215
17 A.P. Murani, *J. Phys. F: Met. Phys*., 1974, **4**, 757
18 F.W. Smith, J.C. Liu, *Solid State Communication*, 1978, **26**, 91
19 B. de Mayo, *J. Phys. Chem. Solids*, 1974, **35**, 1525
20 J. Higgins, P. Wilkes, *Philos. Mag., Ser. 8,* 1972, **25.1**, 599
21 M. Frebel, B. Predel, *Z. Metallkd*., 1973, **64**, 913
22 K.A. Jackson, in "Liquid Metals and Solidification" Cleveland, Ohio: American Society for Metals, 1958, 174
23 D. Cheetham, N. Ridley, *Metall. Trans*., 1973, **4**, 99
24 M. Hillert, in "Decomposition of Austenite by Diffusional Processes" Interscience, New York, 1962, 197
25 H.I. Aaronson, W.B. Triplett, G.M. Andes, *Trans. AIME*, 1957, **209**, 1227
26 G.W. Franti, J.C. Wiliams, H.I. Aaronson, *Metall. Trans*., 1978, **9A**, 1641
27 H.I. Aaronson, W.B. Triplett, G.M. Andes, *Trans. AIME*, 1960, **218**, 331
28 C. W. Spencer, D. J. Mack, in "Decomposition of Austenite by Diffusional Processes" Interscience, New York, 1962, 549
29 A.W. Hassel, B. Bello Rodriguez, S. Milenkovic, A. Schneider, *Electrochim. Acta* 2005, **51**, 795
30 A.W. Hassel, A.J. Smith, S. Milenkovic, *Electrochim. Acta* 52 (2006) 1799.
31 S. Milenkovic, A.W. Hassel, A. Schneider, *Nano Letters 6* (2006) 794.